

# Scattering of massless and massive monopoles in an $SU(N)$ theory

Xingang Chen\* and Erick J. Weinberg†

*Department of Physics  
Columbia University  
New York, NY 10027*

## Abstract

We use the moduli space approximation to study the time evolution of magnetically charged configurations in a theory with an  $SU(N+2)$  gauge symmetry spontaneously broken to  $U(1)\times SU(N)\times U(1)$ . We focus on configurations containing two massive and  $N-1$  massless monopoles. The latter do not appear as distinct objects, but instead coalesce into a cloud of non-Abelian field. We find that at large times the cloud and the massless particles are decoupled, with separately conserved energies. The interaction between them occurs through a scattering process in which the cloud, acting very much like a thin shell, contracts and eventually bounces off the cores of the massive monopoles. The strength of the interaction, as measured, e.g., by the amount of energy transfer, tends to be greatest if the shell is small at the time that it overlaps the massive cores. We also discuss the corresponding behavior for the case of the  $SU(3)$  multimonopole solutions studied by Dancer.

---

\*[xgchen@phys.columbia.edu](mailto:xgchen@phys.columbia.edu)

†[ejw@phys.columbia.edu](mailto:ejw@phys.columbia.edu)

## I. INTRODUCTION

There has long been an interest in the magnetic monopoles that arise as classical solutions in certain spontaneously broken gauge theories. When the theory is quantized, these give rise to magnetically charged particles that can be regarded as the counterparts of the electrically charged elementary quanta of the theory. In certain supersymmetric theories, these two classes of particles are believed to be related by an exact duality symmetry [1].

When the gauge symmetry is spontaneously broken, the gauge bosons corresponding to the generators of the unbroken subgroup remain massless. If the unbroken subgroup contains a non-Abelian factor, some of these massless gauge bosons transform nontrivially under the gauge group and thus carry an “electric” charge. Duality suggests that these should have massless magnetically-charged counterparts. Although these cannot be realized as isolated classical solutions, evidence for their existence can be found by analyzing multimonopole solutions. In this paper we will investigate some of the properties of these massless monopoles by examining the role that they play in low energy scattering processes.<sup>1</sup>

Recall that an arbitrary magnetically charged Bogomol’nyi-Prasad-Sommerfield (BPS) [2] solution can be naturally understood as being composed of a number of fundamental monopoles of various types [3]. If the gauge symmetry  $G$  is broken to an Abelian subgroup  $U(1)^r$ , as happens for generic choices of the adjoint Higgs vacuum expectation value, there is an integer-valued topological charge for each  $U(1)$  factor. Associated to each of these is a fundamental monopole carrying a single unit of that topological charge. Each of these fundamental monopoles can be realized as a classical solution by embedding the unit  $SU(2)$  monopole solution in an appropriate subgroup of  $G$ .

For the special choices of the Higgs vacuum expectation value that give a non-Abelian unbroken subgroup, the BPS mass formula implies that some of the fundamental monopoles should become massless. Although the corresponding embedding solutions reduce to pure vacuum solutions in this limit, analysis of multimonopole solutions suggests that the collective coordinates of the massless fundamental monopoles survive as degrees of freedom. Examining static classical solutions with magnetic charges corresponding to a sum of massive and massless monopoles, one finds that the massive monopoles are surrounded by one or more “clouds” of non-Abelian field [4]. The number of collective coordinates [5] needed to describe these clouds is exactly equal to the number that one would have attributed to

---

<sup>1</sup>Although the underlying motivation for this work arises from theories with extended supersymmetry, this supersymmetry does not come into play at the leading, classical, order to which we work.

the massless monopoles.<sup>2</sup>

To make these ideas more concrete, consider the case of an  $SU(N+2)$  gauge theory with an adjoint Higgs field whose asymptotic value (in some fixed direction) can be brought into the form

$$\Phi = \text{diag}(t_1, t_2, \dots, t_{N+2}) \quad (1.1)$$

with  $t_1 \geq t_2 \geq \dots \geq t_{N+2}$ . The asymptotic magnetic field in the same direction can be written as  $F_{ij} = \epsilon_{ijk} r_k Q_M / r^3$ , where the magnetic charge  $Q_M$  is of the form

$$Q_M = \text{diag}(n_1, n_2 - n_1, \dots, n_{N+1} - n_N, -n_{N+1}) . \quad (1.2)$$

The  $n_k$  are all integers, and give the number of fundamental monopoles of the various types. The mass of the  $k$ th species of fundamental is proportional to  $t_k - t_{k+1}$ . Hence, if the  $t_j$  are all distinct, so that the symmetry is broken maximally, to  $U(1)^{N+1}$ , the  $N+1$  species of fundamental monopoles are all massive. If  $M \geq 2$  of the  $t_k$  are equal, there is an enlarged unbroken symmetry, with  $M-1$  of the  $U(1)$  factors being replaced by an  $SU(M)$ .

We will focus on solutions containing one of each species of monopole, with  $t_1 \neq t_2 = t_3 = \dots = t_{N+1} \neq t_{N+2}$ . The unbroken group is then  $U(1) \times SU(N) \times U(1)$ , and our solutions contain two massive and  $N-1$  massless monopoles. This example has two advantages for us. First, a number of analytic results about the static solutions and their moduli space are already known. Second, because the two massive monopoles correspond to commuting  $SU(2)$  subgroups of the  $SU(N+2)$ , they can have no direct interactions. Any interaction between them must be due to the mediation of the massless monopoles, and thus can give us insight into the properties of the cloud.

Explicit solutions for an  $SU(N+2)$  theory with the  $n_k$  all equal to unity were obtained in Ref. [7]. For either type of symmetry breaking, these solutions are described by  $4(N+1)$  collective coordinates. When the fundamental monopoles are all massive, these have a natural interpretation as the spatial coordinates,  $\mathbf{x}_a$ , and  $U(1)$  phases of the  $N+1$  constituent monopoles; as long as the separation between the monopole positions is large compared to the monopole core sizes, the multimonopole nature of the configuration is evident in the classical solution. As the Higgs field approaches the value corresponding to the non-Abelian breaking,

---

<sup>2</sup>This counting of collective coordinates assumes that the total magnetic charge of the configuration is Abelian. Configurations whose total magnetic charges have non-Abelian components can be regarded as having clouds that have expanded out to spatial infinity, and have a corresponding reduction in the number of collective coordinates. For discussions of some of the pathologies that arise in the presence of non-Abelian magnetic charges, see [6].

monopoles 1 and  $N + 1$ , which remain massive, clearly retain their identity.<sup>3</sup> However, the  $N - 1$  monopoles that become massless are replaced by a single cloud surrounding the massive monopoles; this cloud can be viewed as being formed by the merger of the cores of the massless monopoles. Inside this cloud, the magnetic field is approximately equal to the the Coulomb field appropriate to the charges of the massive monopoles; it has both Abelian and non-Abelian components. Outside the cloud, the Coulomb component of the magnetic field is purely Abelian, with the non-Abelian contributions falling with a higher power of distance.

The size of this cloud is characterized by a “cloud parameter”  $b$  that is equal to the sum of the separations  $|\mathbf{x}_a - \mathbf{x}_{a+1}|$  between the monopoles. Any value  $b \geq r \equiv |\mathbf{x}_1 - \mathbf{x}_{N+1}|$ , the separation of the two massive monopoles, is possible, and the static energy is independent of  $b$ . All other trace of the massless monopole positions appears to be lost in this limit. In particular, the fields show no special behavior at the  $\mathbf{x}_a$  corresponding to the massless monopoles. In fact, any change in these “positions” that leaves  $b$  invariant can be compensated by a gauge transformation of the solution.

Our goal in this paper is to gain further insight into the nature of these massless monopoles by examining the role that the cloud plays in monopole scattering. To do this we use the moduli space approximation [8], which reduces the dynamics of the infinite number of field degrees of freedom to that of a finite number of collective coordinates  $q_i$ . The Lagrangian for this reduced set of variables can be written as

$$L = \frac{1}{2} g_{ij}(q) \dot{q}^i \dot{q}^j \quad (1.3)$$

where

$$\mathcal{G} = g_{ij}(q) dq^i dq^j \quad (1.4)$$

is a naturally defined metric on the moduli space of solutions. The evolution of the collective coordinates is simply geodesic motion in this metric. When the monopoles are all massive, this reduction to a finite number of degrees of freedom fits quite well with the point of view that particles arising from classical soliton solutions should be seen as having a similar status to those arising as quanta of the elementary fields, and that the solutions with higher charge should be interpreted as multiparticle states. When some of the monopoles become massless, the classical solutions lose their manifest multiparticle nature. Nevertheless, the

---

<sup>3</sup>We label the component monopoles by the particular magnetic charge that they carry; thus monopole  $a$  has  $n_a = 1$  and corresponds to an  $SU(2)$  embedding in the  $a$  and  $a + 1$  rows and columns of the  $SU(N + 2)$  matrices.

massless monopole collective coordinates survive (although with their physical interpretations modified) and the moduli space Lagrangian has a smooth limit [9], provided that the total magnetic charge is Abelian.

The moduli space approximation is usually expected to be valid in the limit of small monopole velocities. This ensures that the monopole kinetic energy is small enough that the excitation of the nonzero-frequency modes of the massive fields is energetically suppressed. Although simple energetic arguments are not sufficient to rule out excitation of any massless fields that might be present, more detailed analysis [10] shows that the approximation holds if the long-range fields are all Abelian. As we will see, the situation with massless non-Abelian fields is more complex.

To use the moduli space approximation, we need the metric on the space of multi-monopole solutions. The exact form of this metric is known for only a relatively few cases. However, these include [12,13] the case where there is at most one of each species of fundamental monopole, which is precisely what we need. Unfortunately, the form of this metric that was obtained in Ref. [12] was expressed in terms of the positions and  $U(1)$  phases of the  $(N + 1)$  individual monopoles. Although these are the natural coordinates to use when the monopoles are all massive, they are much less useful in the limit we are interested in, where the massless monopole positions have little direct physical meaning. A more natural set of coordinates would include the positions and  $U(1)$  phases of the two massive monopoles, the cloud parameter  $b$ , and the parameters needed to specify the global  $SU(N)$  orientation of the cloud.

Thus, our first task is to change to a new set of variables. We do this in two steps. In Sec. II we transform to an intermediate set of coordinates that allows us to separate the metric into two parts, one that gives the terms in the Lagrangian containing  $\dot{r}$  and  $\dot{b}$ , and an “angular” part that contains the entire dependence on the spatial and gauge orientation angles and phases. The natural next step would be to relate these intermediate coordinates to the spatial Euler angles and their gauge counterparts. This turns out to be somewhat nontrivial. However, we can bypass this step by rephrasing the problem in terms of the corresponding angular momenta and charges. We do this in Sec. III, leaving the discussion of the Euler angles to the Appendix. With these results in hand, we are then ready to determine the geodesics of the metric and the behavior of the monopoles in scattering processes. This is described in Sec. IV. We summarize our results and make some concluding remarks in Sec. V.

## II. THE MODULI SPACE METRIC

The moduli space of solutions for a system comprising two distinct fundamental monopoles was obtained in Ref. [11]; the extension to any number of distinct monopoles was conjectured in Ref. [12] and proven in Ref. [13]. Locally, this space can be written as a product of a flat 4-dimensional space, corresponding to the center-of-mass position and an overall U(1) variable, and a relative moduli space. For the case of interest to us, an SU( $N+2$ ) theory with one monopole of each species, the moduli space is  $4(N+1)$ -dimensional, and the  $4N$  coordinates for the relative moduli space can be chosen to be the relative positions  $\mathbf{r}_A = \mathbf{x}_A - \mathbf{x}_{A+1}$  ( $A = 1, 2, \dots, N$ ) and the corresponding relative U(1) phases  $\psi_A$ .

In Ref. [9] it was shown that when the SU( $N+2$ ) symmetry is broken to U(1) $\times$ SU( $N$ ) $\times$ U(1) this metric can be written as

$$\mathcal{G}_{\text{rel}} = \mu \left[ \sum_A d\mathbf{r}_A \right]^2 + \kappa \sum_A \left[ \frac{1}{r_A} d\mathbf{r}_A^2 + r_A (d\psi_A + \cos \theta_A d\phi_A)^2 \right] - \lambda \left[ \sum_A r_A (d\psi_A + \cos \theta_A d\phi_A) \right]^2 \quad (2.1)$$

where  $r_A$ ,  $\theta_A$ , and  $\phi_A$  are the spherical coordinates of the vector  $\mathbf{r}_A$ ,  $\mu$  is the reduced mass of the two massive monopoles, and

$$\begin{aligned} \kappa &= \frac{g^2}{8\pi} \\ \lambda &= \frac{g^2 \mu}{g^2 + 8\pi \mu b} = \mu \left[ \frac{r_c}{2b + r_c} \right]. \end{aligned} \quad (2.2)$$

Here  $g = 4\pi/e$  (with  $e$  the gauge coupling of the theory) is the magnitude of the fundamental monopole magnetic charge, while  $r_c \equiv 2\kappa/\mu$  is approximately equal to the sum of the core radii of the two massive monopoles.

The difficulty with using this expression for our purposes is that, as we noted in Sec. I, the positions of the massless monopoles do not have any direct physical meaning. We would therefore like to transform to a more physically meaningful set of variables. This set should include the cloud parameter  $b$  and the spherical coordinates  $r$ ,  $\theta$ , and  $\phi$  of the vector  $\mathbf{r}$  that gives the relative separation of the two massive monopoles, but must also include the relative U(1) phase and a number of SU( $N$ ) orientation angles.

One might expect that  $N^2 - 1 = \dim[\text{SU}(N)]$  such angles would be needed to specify the gauge orientation of the solution. For  $N > 2$  this would require more collective coordinates than are available. However, examination of the explicit solutions shows that there is always a U( $N-2$ ) subgroup of the unbroken SU( $N$ ) that leaves the fields invariant [i.e., any of these SU( $N+2$ ) solutions is essentially an embedding of an SU(4) solution]. Hence, there are only  $4N - 5 = \dim[\text{SU}(N)/\text{U}(N-2)]$  global SU( $N$ ) parameters. Together with the

U(1) phases, the cloud size  $b$ , and the positions of the two massive monopoles, this gives a total of  $4(N + 1)$  collective coordinates, as required.

We begin by defining complex coordinates<sup>4</sup>

$$\begin{aligned} z_A^1 &= \sqrt{r_A} \cos(\theta_A/2) e^{-i(\phi_A + \psi_A)/2} \\ z_A^2 &= \sqrt{r_A} \sin(\theta_A/2) e^{i(\phi_A - \psi_A)/2} . \end{aligned} \quad (2.3)$$

These satisfy

$$\mathbf{r}_A = \bar{z}_A^a (\boldsymbol{\sigma})_{ab} z_A^b \quad (2.4)$$

where  $\bar{z}_A^a = (z_A^a)^*$  and the  $\sigma_k$  are the Pauli matrices. Hence, the relative position of the two massive monopoles is<sup>5</sup>

$$\mathbf{r} = \bar{z} \boldsymbol{\sigma} z \quad (2.5)$$

while

$$b = \bar{z} z . \quad (2.6)$$

When rewritten in terms of these coordinates, the metric takes the form

$$\begin{aligned} \mathcal{G}_{\text{rel}} &= \mu [\bar{z} \boldsymbol{\sigma} dz + d\bar{z} \boldsymbol{\sigma} z]^2 + 4\kappa d\bar{z} dz + \lambda [\bar{z} dz - d\bar{z} z]^2 \\ &= \mu d\mathbf{r}^2 + 4\kappa d\bar{z} dz + \lambda [\bar{z} dz - d\bar{z} z]^2 . \end{aligned} \quad (2.7)$$

Next, we find an SU(2) matrix  $U$  satisfying

$$U \hat{\mathbf{r}} \cdot \boldsymbol{\sigma} U^{-1} = \sigma_3 \quad (2.8)$$

where  $\hat{\mathbf{r}} = \mathbf{r}/r$ . (Thus,  $U$  corresponds to a rigid rotation of the entire assembly of monopoles that puts the two massive monopoles on the  $z$ -axis.) This allows us to define a new set of complex variables

$$w_A^a = U_{ab} z_A^b \quad (2.9)$$

in terms of which  $r$  and  $b$  are given by the simple expressions

$$\bar{w} \sigma_j w = r \delta_{j3} , \quad \bar{w} w = b . \quad (2.10)$$

---

<sup>4</sup>In the notation of Ref. [9],  $z_A^1 = \xi_A/2$  and  $z_A^2 = \zeta_A^*/2$ .

<sup>5</sup>Omitted indices on the  $z_A^a$  and related quantities should be understood as being summed over.

These identities imply that the  $w_A^a$  must be of the form

$$\begin{aligned} w_A^1 &= \sqrt{\frac{b+r}{2}} p_A^{(1)} \\ w_A^2 &= \sqrt{\frac{b-r}{2}} p_A^{(2)} \end{aligned} \quad (2.11)$$

where the  $p_A^{(a)}$  are a pair of complex  $N$ -component vectors obeying

$$\bar{p}_A^{(a)} p_A^{(b)} = \delta_{ab} . \quad (2.12)$$

For later use, we also introduce  $N - 2$  orthonormal vectors  $e_A^{(r)}$  ( $r = 3, 4, \dots, N$ ) orthogonal to the  $p_A^{(a)}$ .

We must now rewrite the metric in terms of these new variables. It will be helpful to introduce some new notation. First, we define two unit vectors  $\hat{\mathbf{n}}_1$  and  $\hat{\mathbf{n}}_2$  orthogonal to  $\hat{\mathbf{r}}$  by requiring that

$$U \hat{\mathbf{n}}_a \cdot \boldsymbol{\sigma} U^{-1} = \sigma_a . \quad (2.13)$$

Next, we define  $A_j$  and  $V_j$  ( $j = 1, 2, 3$ ) by

$$dU U^{-1} = -\frac{1}{2i} A_j \sigma_j \quad (2.14)$$

and

$$V_j = i[\bar{w} \sigma_j dw - d\bar{w} \sigma_j w] . \quad (2.15)$$

Finally, we define

$$V_0 = i[\bar{w} dw - d\bar{w} w] . \quad (2.16)$$

We also need two identities. First, by differentiating both sides of Eq. (2.8), one is led to

$$d\mathbf{r} = \hat{\mathbf{r}} dr + r(\hat{\mathbf{n}}_1 A_2 - \hat{\mathbf{n}}_2 A_1) . \quad (2.17)$$

Next, viewing the  $w^a$  as vectors in an  $N$ -dimensional complex vector space, we write

$$d\bar{w} dw = d\bar{w}_A^a [\Pi_{AB}^L + \Pi_{AB}^T] dw_B^a \quad (2.18)$$

where

$$\Pi_{AB}^L = \sum_{a=1}^2 p_B^{(a)} \bar{p}_A^{(a)} \quad (2.19)$$



is the projection operator onto the two-dimensional subspace spanned by  $w^1$  and  $w^2$  (or by  $z^1$  and  $z^2$ ) and

$$\Pi_{AB}^T = \sum_{r=3}^N e_A^{(r)} \bar{e}_B^{(r)} . \quad (2.20)$$

is the projection operator onto the orthogonal  $(N - 2)$ -dimensional subspace. Using Eqs. (2.10), (2.11), (2.15), and (2.16), we obtain the second identity,

$$d\bar{w} dw = \frac{[d(b+r)]^2}{8(b+r)} + \frac{[d(b-r)]^2}{8(b-r)} + \frac{b}{4(b^2-r^2)} \sum_{\nu=0}^3 V_\nu^2 - \frac{r}{2(b^2-r^2)} (V_0 V_3) + d\bar{w} \Pi^T dw . \quad (2.21)$$

We have not yet obtained explicit expressions for  $\theta$ ,  $\phi$ , or the gauge orientation phases in terms of the  $w_A^a$  or  $U$ . However, it is easy to see that neither the  $A_i$  and  $V_\nu$  nor the combination  $d\bar{w} \Pi^T dw$  can contain any factors of  $dr$  or  $db$ . With this in mind, and using our two identities and the above definitions, we substitute Eq. (2.9) into Eq. (2.7) and obtain

$$\mathcal{G}_{\text{rel}} = \mu dr^2 + \kappa \left\{ \frac{[d(b+r)]^2}{2(b+r)} + \frac{[d(b-r)]^2}{2(b-r)} \right\} + \mathcal{G}_{\text{ang}} \quad (2.22)$$

where

$$\begin{aligned} \mathcal{G}_{\text{ang}} = & \sum_{i=1}^2 \left[ \mu r^2 A_i^2 + \frac{\kappa b}{b^2 - r^2} V_i^2 + \kappa (2A_i V_i + bA_i^2) \right] + \left( \frac{\kappa b}{b^2 - r^2} - \lambda \right) (V_0 + rA_3)^2 \\ & + \frac{\kappa b}{b^2 - r^2} (V_3 + bA_3)^2 - \frac{2\kappa r}{b^2 - r^2} (V_0 + rA_3)(V_3 + bA_3) + 4\kappa d\bar{w} \Pi^T dw \end{aligned} \quad (2.23)$$

contains the entire dependence of the metric on the spatial angles and the various gauge orientation phases. In the next section we will rewrite  $\mathcal{G}_{\text{ang}}$  in a form that will allow us to analyze the evolution of these angle and gauge variables.

Before doing so, we comment on a point that we have skipped over. Equation (2.8) does not completely determine the matrix  $U$ , but instead leaves the freedom to make a further transformation of the form

$$U \longrightarrow e^{i\chi\sigma_3/2} U . \quad (2.24)$$

This implies a corresponding transformation

$$w \longrightarrow e^{i\chi\sigma_3/2} w \quad (2.25)$$

of the  $w_A^a$ , and rotates the unit vectors  $\hat{\mathbf{n}}_1$  and  $\hat{\mathbf{n}}_2$  so that

$$\hat{\mathbf{n}}_1 + i\hat{\mathbf{n}}_2 \longrightarrow e^{-i\chi} (\hat{\mathbf{n}}_1 + i\hat{\mathbf{n}}_2) . \quad (2.26)$$

This ambiguity in the definition of  $U$  is not simply due to our failure to impose a sufficient number of conditions. Instead, it reflects the fact that these solutions possess an axial symmetry. They are invariant under rotations about the axis joining the two massive monopoles, provided that these are combined with an appropriate global gauge transformation. Because of this symmetry, there is no natural way to pick out any particular pair of axes in the plane perpendicular to  $\hat{\mathbf{r}}$ . As a result, the form of the metric should be invariant under such redefinitions of  $U$ . To verify that it is, we note that the auxiliary quantities  $A_i$  and  $V_\nu$  transform as

$$\begin{aligned}
A_1 + iA_2 &\longrightarrow e^{-i\chi}(A_1 + iA_2) \\
A_3 &\longrightarrow A_3 + d\chi \\
V_1 + iV_2 &\longrightarrow e^{-i\chi}(V_1 + iV_2) \\
V_3 &\longrightarrow V_3 - b d\chi \\
V_0 &\longrightarrow V_0 - r d\chi .
\end{aligned} \tag{2.27}$$

Substituting these results into Eq. (2.23), we see that the metric is indeed unchanged, thus providing a useful consistency check on our calculations.

### III. ANGLES, PHASES, AND CONSERVED QUANTITIES

In this section we will bring Eq. (2.23) for  $\mathcal{G}_{\text{ang}}$  into a form more suitable for analyzing the dynamics of the angle and phase variables. The most straightforward method for doing this would begin by defining generalized Euler angles to describe the spatial and the  $U(N)$  phase orientations. Given these, one can construct a set of 1-forms  $\omega^j$  invariant under both the spatial  $SO(3)$  and the internal  $SU(N)$  symmetries of the theory, and write

$$\mathcal{G}_{\text{ang}} = I_{ij}(r, b)\omega^i\omega^j . \tag{3.1}$$

The symmetries of the system imply the existence of a conserved angular momentum and conserved  $U(N)$  charges. The “body-frame” components of these quantities, defined by

$$X_i dt = I_{ij}(r, b)\omega^j \tag{3.2}$$

are the variables conjugate to the invariant one-forms. Writing

$$\mathcal{G}_{\text{ang}} = (I^{-1})^{ij}(r, b)X_i X_j dt^2 \tag{3.3}$$

and then substituting this into Eq. (2.22) gives a convenient starting point for studying the dynamics of the system.

A complication in our case is that, because of the extra symmetries of these multi-monopole solutions, the number of angular variables is less than might be expected. For

most choices of the magnetic charges, an arbitrary configuration would require 3 spatial Euler angles and  $N^2$  phases specifying the  $U(N)$  orientation. By contrast, the relative moduli space in our case is  $4N$ -dimensional so that, after extracting  $r$  and  $b$ , we are left with only  $4N - 2$  angle and phase variables. The “missing”  $(N - 2)^2 + 1$  variables are explained by extra invariances of the solutions we are considering. First, we noted previously, these  $SU(N + 2)$  solutions are essentially equivalent to embeddings of  $SU(4)$  solutions, so that there is always a  $U(N - 2)$  subgroup that leaves the configuration invariant.<sup>6</sup> The  $(N - 2)^2$  “Euler angles” corresponding to this subgroup play no role in the dynamics, and hence do not enter the Lagrangian. Second, the axial symmetry discussed at the end of the previous section implies that some linear combination of a spatial Euler angle and a  $U(N)$  phase must also be absent from the metric.<sup>7</sup>

The fact that these extra symmetries involve mixtures of spatial rotations and gauge transformations complicates the explicit construction of the  $\omega^i$  appearing in Eq. (3.1); they are not simply subsets of the standard invariant one-forms for  $SO(3)$  and  $U(N)$ . Fortunately, it turns out that we can bypass the construction of the  $\omega^i$  and go directly from Eq. (2.23) to an expression of the form given in Eq. (3.3). We will follow this procedure in this section, leaving the discussion of the generalized Euler angles and the  $\omega^i$  to the Appendix.

We begin by identifying the conserved quantities of the system. Recall that if a metric has a Killing vector of the form

$$K_{(i)} = K_{(i)}^a \frac{\partial}{\partial q^a} \tag{3.4}$$

then the charge

$$Q_{(i)} = K_{(i)}^a \dot{q}_a = g_{ab} K_{(i)}^a \dot{q}^b \tag{3.5}$$

is a constant along any geodesic. Since the classical solutions of the moduli space Lagrangian are all geodesics, these  $Q_{(i)}$  are the desired conserved charges.

---

<sup>6</sup>Note, however, that the particular  $U(N - 2)$  subgroup depends on the  $SU(N)$  orientation of the configuration, and thus changes as the various phases vary with time.

<sup>7</sup>The apparent analogy between a rigid body symmetric top and our axially symmetric field configurations is a bit misleading. In the former case, time-dependent rotations about the symmetry axis are physically meaningful and have kinetic energy associated with them. Although the rotation angle about this axis does not appear in the Lagrangian, its time derivative does. In our case, such rotations, whether time-dependent or not, are undetectable and have no associated kinetic energy. Thus, the best analogue is not an ordinary symmetric top with principle moments of inertia  $I_1 = I_2 \neq I_3 \neq 0$ , but rather an infinitely thin top with  $I_1 = I_2$  and  $I_3 = 0$ .

The Killing vectors of the metric of Eq. (2.1) were determined in Ref. [9]. Written in terms of our complex variables  $z_A^a$ , the rotational Killing vectors take the form

$$L_k = \frac{i}{2} \left[ z_A^b (\sigma_k)_{ab} \frac{\partial}{\partial z_A^a} - \bar{z}_A^b (\sigma_k)_{ba} \frac{\partial}{\partial \bar{z}_A^a} \right] \quad (3.6)$$

while the  $N^2$  Killing vectors

$$E_{AB} = \frac{i}{\sqrt{2}} \left[ z_A^a \frac{\partial}{\partial z_B^a} - \bar{z}_B^a \frac{\partial}{\partial \bar{z}_A^a} \right] \quad (3.7)$$

satisfy the algebra of  $U(N)$ .

Using Eqs.(3.4) and (3.5), we construct from these the angular momentum

$$\begin{aligned} \mathbf{J} dt &= \mu (\bar{z} \boldsymbol{\sigma} z) \times [\bar{z} \boldsymbol{\sigma} dz + d\bar{z} \boldsymbol{\sigma} z] + i\kappa [\bar{z} \boldsymbol{\sigma} dz - d\bar{z} \boldsymbol{\sigma} z] - i\lambda [\bar{z} dz - d\bar{z} z] (\bar{z} \boldsymbol{\sigma} z) \\ &= \mu \mathbf{r} \times d\mathbf{r} + \kappa \left[ i(\bar{w} U \boldsymbol{\sigma} U^{-1} dw - d\bar{w} U \boldsymbol{\sigma} U^{-1} w) + i\bar{w} (\mathcal{A} U \boldsymbol{\sigma} U^{-1} + U \boldsymbol{\sigma} U^{-1} \mathcal{A}) w \right] \\ &\quad - \lambda \mathbf{r} (V_0 + rA_3) \end{aligned} \quad (3.8)$$

(where  $\mathcal{A} = A_j \sigma_j$ ) and the  $U(N)$  charges

$$\begin{aligned} \mathcal{E}_{AB} dt &= i\sqrt{2}\kappa [d\bar{z}_B z_A - \bar{z}_B dz_A] + i\lambda \bar{z}_B z_A [\bar{z} dz - d\bar{z} z] \\ &= \sqrt{2}\kappa [i(d\bar{w}_B w_A - \bar{w}_B dw_A - \bar{w}_B \sigma_j w_A A_j) + \sqrt{2}\lambda \bar{w}_B w_A (V_0 + rA_3)] . \end{aligned} \quad (3.9)$$

The components implied by the bold-face notation in Eq. (3.8) and by the subscripts in Eq. (3.9) are those corresponding to a fixed “space-frame” and are conserved. What we actually need are the components corresponding to a moving “body-frame”. For the angular momentum, this requires identifying three axes that rotate with the monopole system; a suitable choice is  $\hat{\mathbf{n}}_1$ ,  $\hat{\mathbf{n}}_2$ , and  $\hat{\mathbf{n}}_3 \equiv \hat{\mathbf{r}}$ . The body frame components (which are themselves rotational scalars) are then

$$J_i dt \equiv \hat{\mathbf{n}}_i \cdot \mathbf{J} dt = \begin{cases} (\mu r^2 + \kappa b) A_i + \kappa V_i & i = 1, 2 \\ -r\lambda(V_0 + rA_3) + \kappa(V_3 + bA_3) & i = 3 \end{cases} . \quad (3.10)$$

In obtaining this, we have used Eqs. (2.13) and (2.15).

To construct a “body-frame” for the  $U(N)$  charges, we need a set of  $N$  complex basis vectors in the internal space that transform under the fundamental representation under the action of the  $\mathcal{E}_{AB}$ . We can take these to be the  $p_A^{(a)}$  and the  $e_A^{(r)}$  that were introduced in Sec. 2. Using the  $p_A^{(a)}$  and the Pauli matrices, we can construct three  $U(N)$ -invariant charges

$$T_k = \frac{1}{\sqrt{2}} \bar{p}_A^{(a)} [\tau_k]_{ab} p_B^{(b)} \mathcal{E}_{AB} . \quad (3.11)$$

(The definition of these has been chosen so that they correspond to generators of an SU(2) subgroup with the standard normalization.) Straightforward calculations give

$$T_i dt = \begin{cases} \kappa \left[ \frac{b}{\sqrt{b^2 - r^2}} V_i + \sqrt{b^2 - r^2} A_i \right] & i = 1, 2 \\ r\lambda(V_0 + rA_3) - \kappa(V_3 + bA_3) & i = 3 \end{cases} . \quad (3.12)$$

Comparing Eqs. (3.10) and (3.12), we see that

$$J_3 + T_3 = 0 \quad (3.13)$$

which is a reflection of the axial symmetry of the solutions.

Additional “body-frame” components can be constructed by utilizing contractions with the  $e_A^{(r)}$ . Components involving two such contractions vanish; i.e.,<sup>8</sup>

$$\bar{e}_A^{(r)} e_B^{(s)} \mathcal{E}_{AB} = 0 . \quad (3.14)$$

On the other hand, the charges

$$t_{ar} = \bar{p}_A^{(a)} e_B^{(r)} \mathcal{E}_{AB} \quad (3.15)$$

and their complex conjugates  $\bar{t}_{ar}$  are in general nonzero; they are related to the last term in Eq. (2.23) by

$$\frac{d\bar{w}}{dt} \Pi^T \frac{dw}{dt} = \frac{1}{\kappa^2} \sum_{r=3}^N \left[ \frac{t_{1r} \bar{t}_{1r}}{b+r} + \frac{t_{2r} \bar{t}_{2r}}{b-r} \right] . \quad (3.16)$$

Finally, we define a conserved relative U(1) charge

$$\begin{aligned} Q dt &= \frac{1}{\sqrt{2}} \mathcal{E}_{AA} dt = \frac{1}{\sqrt{2}} \left[ \Pi_{AB}^T + \Pi_{AB}^L \right] \mathcal{E}_{AB} dt = \frac{1}{\sqrt{2}} \sum_{a=1}^2 p_B^{(a)} \bar{p}_A^{(a)} \mathcal{E}_{AB} dt \\ &= (b\lambda - \kappa)(V_0 + rA_3) . \end{aligned} \quad (3.17)$$

Using Eqs. (2.23), (3.10), (3.12), (3.16), and (3.17), we can now rewrite  $\mathcal{G}_{\text{ang}}$  in terms of the body-frame components, obtaining

$$\begin{aligned} \mathcal{G}_{\text{ang}} &= \left\{ \frac{1}{r^2(\kappa + \mu b)} \sum_{i=1}^2 \left[ bJ_i^2 + \left( b + \frac{\mu r^2}{\kappa} \right) T_i^2 - 2\sqrt{b^2 - r^2} J_i T_i \right] \right. \\ &\quad \left. + \frac{1}{\kappa(b^2 - r^2)} \left[ b(J_3^2 + Q^2) + 2rJ_3Q \right] + \frac{\mu}{\kappa^2} Q^2 + \frac{4}{\kappa} \sum_{r=3}^N \left[ \frac{t_{1r} \bar{t}_{1r}}{b+r} + \frac{t_{2r} \bar{t}_{2r}}{b-r} \right] \right\} dt^2 . \end{aligned} \quad (3.18)$$

---

<sup>8</sup>This is just a restatement of the fact that  $(N-2)^2$  eigenvalues of the moment of inertia tensor vanish because of invariance under a U( $N-2$ ) subgroup.

It must be remembered that the “body frame” components that appear in this expression are not in general conserved. While the square of the angular momentum,

$$\mathbf{J}^2 = J_1^2 + J_2^2 + J_3^2 \quad (3.19)$$

the  $SU(N)$  Casimir,

$$T^2 = T_1^2 + T_2^2 + T_3^2 + \sum_{r=3}^N (t_{1r} \bar{t}_{1r} + t_{2r} \bar{t}_{2r}) \quad (3.20)$$

and the  $U(1)$  charge  $Q$  are constant, determining the time-dependence of the individual components of  $\mathbf{J}$  and  $T$  is in general rather complex. There is considerable simplification, however, if the  $SU(N)$  charges all vanish. The only nonzero charges remaining are then  $J_1$ ,  $J_2$ , and  $Q$ , with the former two entering  $\mathcal{G}_{\text{ang}}$  only through  $\mathbf{J}^2 = J_1^2 + J_2^2$ ; using the relation between  $V_i$  and  $A_i$  that follow from the vanishing of the  $T_i$ , one finds that this is given by

$$\mathbf{J}^2 = \left( \mu + \frac{\kappa}{b} \right)^2 r^4 (\dot{\theta}^2 + \sin^2 \theta \dot{\phi}^2) . \quad (3.21)$$

Equation (3.18) then reduces to

$$\mathcal{G}_{\text{ang}}(T = 0) = \left\{ \frac{b\mathbf{J}^2}{r^2(\kappa + \mu b)} + \left[ \frac{\mu}{\kappa^2} + \frac{b}{\kappa(b^2 - r^2)} \right] Q^2 \right\} dt^2 . \quad (3.22)$$

#### IV. MONOPOLE TRAJECTORIES

We are now ready to obtain the equations of motion of our system and study the behavior of the cloud and the massive monopoles in scattering processes. We restrict ourselves here to the case of vanishing  $SU(N)$  charges,  $T = 0$ , leaving a discussion of the more general case to the Appendix.

Because the massive monopoles have well-defined positions while the massless ones do not, there may be a tendency to view the various scattering processes as resulting from interactions between the massive monopoles, with the cloud dynamics being in the background. This would be incorrect. The massive monopoles correspond to two mutually commuting  $SU(2)$  subgroups of  $SU(N + 2)$ . Were it not for the presence of the cloud, they would not interact at all and would move on straight lines with constant velocity. Hence, when following the motion of the massive monopoles it is important to also keep track of the size and motion of the cloud at the same time.

Equations (2.22) and (3.22) provide a suitable starting point for obtaining the equations of motion of our system. Because the angle and phase variables enter the latter only through

conserved quantities, we can view  $\mathcal{G}_{\text{ang}}$  as defining an effective potential for  $r$  and  $b$  that can be combined with the first two terms in Eq. (2.22) to yield an effective Lagrangian<sup>9</sup>

$$L_{\text{eff}} = \frac{\mu}{2}\dot{r}^2 + \frac{\kappa}{4} \left[ \frac{(\dot{b} + \dot{r})^2}{b+r} + \frac{(\dot{b} - \dot{r})^2}{b-r} \right] - \frac{b\mathbf{J}^2}{2r^2(\kappa + \mu b)} - \frac{bQ^2}{2\kappa(b^2 - r^2)}. \quad (4.1)$$

We begin our analysis of the solutions of this Lagrangian by examining the asymptotic solutions at large  $r$  and  $b$ ; because the terms containing  $\mathbf{J}$  and  $Q$  both fall rapidly in this regime, it is sufficient to do this asymptotic analysis with  $\mathbf{J} = Q = 0$ . We find that the cloud and the massive monopoles decouple from each other at large times. After studying the properties of these asymptotic solutions, we then turn to the behavior at finite time, where the actual interactions take place, beginning with  $\mathbf{J} = Q = 0$ . Finally, we consider the effects of nonzero  $\mathbf{J}$  and  $Q$ .

Before beginning this analysis, we must address the apparent singularity in the kinetic energy at  $r = b$ . This singularity is not physical, and can be eliminated by defining

$$\begin{aligned} x &= \sqrt{\kappa} \left[ \sqrt{b+r} + \sqrt{b-r} \right] \\ y &= \sqrt{\kappa} \left[ \sqrt{b+r} - \sqrt{b-r} \right] \end{aligned} \quad 0 \leq y \leq x. \quad (4.2)$$

In terms of these coordinates, the Lagrangian takes the nonsingular form

$$L = \frac{1}{2}(\dot{x}^2 + \dot{y}^2) + \frac{1}{2a^2}(xy + y\dot{x})^2 - \frac{a^2(x^2 + y^2)}{2x^2y^2(a^2 + x^2 + y^2)}\mathbf{J}^2 - \frac{2(x^2 + y^2)}{(x^2 - y^2)^2}Q^2 \quad (4.3)$$

where

$$a = \frac{2\kappa}{\sqrt{\mu}}. \quad (4.4)$$

As we have indicated in Eq. (4.2), the entire physical range  $0 \leq r \leq b < \infty$  is mapped onto the octant  $0 \leq y \leq x$  of the  $x$ - $y$  plane. Nevertheless, it will become clear that if either  $\mathbf{J}$  or  $Q$  vanish some trajectories can cross the boundaries of this octant. These can be understood as follows. The  $x$ -axis corresponds to  $r = 0$ . A trajectory crossing this line corresponds to a motion in which the two massive monopoles approach head-on, meet (at  $y = 0$ ), and then pass through one another. To accommodate this, we extend the definition of  $x$  and  $y$  into the next octant by

$$\begin{aligned} x &= \sqrt{\kappa} \left[ \sqrt{b-r} + \sqrt{b+r} \right] \\ y &= \sqrt{\kappa} \left[ \sqrt{b-r} - \sqrt{b+r} \right] \end{aligned} \quad 0 \leq -y \leq x. \quad (4.5)$$

---

<sup>9</sup>We omit the term  $(\mu/\kappa^2)Q^2$ , which gives a  $Q$ -dependent increase in energy but has no effect on the evolution of  $b$  or  $r$ .

Similarly, a trajectory crossing the line  $x = y$  corresponds to a motion in which the cloud shrinks to its minimum size,  $b = r$ , and then begins to grow again. To describe this, we define

$$\begin{aligned} x &= \sqrt{\kappa} \left[ \sqrt{b+r} - \sqrt{b-r} \right] \\ y &= \sqrt{\kappa} \left[ \sqrt{b+r} + \sqrt{b-r} \right] \end{aligned} \quad 0 \leq x \leq y . \quad (4.6)$$

Extending these definitions in a similar fashion to the other octants, we obtain an eight-fold mapping of the physical  $r$ - $b$  space onto the  $x$ - $y$  plane. Throughout the plane we have the relations

$$\begin{aligned} r &= \frac{1}{2\kappa} |xy| \\ b &= \frac{1}{4\kappa} (x^2 + y^2) \end{aligned} \quad (4.7)$$

so that the  $x$ - and  $y$ -axes correspond to  $r = 0$  while the lines  $y = \pm x$  correspond to minimum cloud size,  $b = r$ .

#### A. Asymptotic solutions for $\mathbf{J} = Q = 0$

If  $\mathbf{J} = Q = 0$  the Lagrangian of Eq. (4.3) reduces to

$$L = \frac{1}{2}(\dot{x}^2 + \dot{y}^2) + \frac{1}{2a^2}(x\dot{y} + y\dot{x})^2 . \quad (4.8)$$

The resulting Euler-Lagrange equations are

$$\begin{aligned} 0 &= (a^2 + y^2)\ddot{x} + xy\ddot{y} + 2y\dot{x}\dot{y} \\ 0 &= (a^2 + x^2)\ddot{y} + xy\ddot{x} + 2x\dot{x}\dot{y} . \end{aligned} \quad (4.9)$$

Multiplying the first of these by  $x$  and the second by  $y$ , and then subtracting, we find that  $x\ddot{x} = y\ddot{y}$ . Using this to rewrite Eq. (4.9), we obtain

$$\begin{aligned} 0 &= (a^2 + x^2 + y^2)\ddot{x} + 2y\dot{x}\dot{y} \\ 0 &= (a^2 + x^2 + y^2)\ddot{y} + 2x\dot{x}\dot{y} . \end{aligned} \quad (4.10)$$

There are two constants of the motion. The time-independence of the Lagrangian implies the conservation of the energy (which is actually equal to the Lagrangian)

$$E = \frac{1}{2}(\dot{x}^2 + \dot{y}^2) + \frac{1}{2a^2}(x\dot{y} + y\dot{x})^2 . \quad (4.11)$$

In addition, multiplication of the first of Eq. (4.10) by  $\dot{y}$  and the second by  $\dot{x}$  shows that



$$B = \frac{1}{a^2} \dot{x} \dot{y} (a^2 + x^2 + y^2) \quad (4.12)$$

is also conserved. (We have no deep understanding as to why  $B$  is constant; we have not found any generalization of  $B$  that is conserved when either  $\mathbf{J}$  or  $Q$  is nonzero.)

If  $B \neq 0$ , neither  $\dot{x}$  nor  $\dot{y}$  can vanish, implying that both  $x$  and  $y$  vary monotonically; if  $B = 0$  but  $E \neq 0$ , then one of  $\dot{x}$  or  $\dot{y}$  vanishes for all  $t$ , while the other never vanishes. Hence, there are no closed orbits in the  $x$ - $y$  plane. It is then straightforward to show that  $x^2 + y^2$  must tend to infinity as  $t \rightarrow \pm\infty$ . There are two possibilities for the large time behavior. The first is that  $dy/dx$  tends to a nonzero finite constant. Examination of Eq. (4.10) shows that this is possible only if  $dy/dx \rightarrow \pm 1$ , which can only happen if  $E = \pm B$ . This gives solutions where  $x^2 = y^2$  varies linearly with time, corresponding to a solution with a minimal ( $b = r$ ) cloud surrounding two massive monopoles with constant relative velocity.

The other possibility is that  $|dy/dx|$  tends to either 0 or  $\infty$ ; because of the eight-fold mapping of  $b$  and  $r$  onto the  $x$ - $y$  plane, the two are equivalent. We will analyze in detail the case where  $dy/dx \rightarrow 0$ , so that asymptotically  $|x| \gg |y|$ . By integrating the dominant terms in the second of Eq. (4.10), we find that  $\dot{y}x^2$  asymptotically tends to a constant. Substituting this result into Eq. (4.12) for  $B$ , we see that  $\dot{x}$  must tend to a constant. It is then straightforward to obtain the asymptotic solution

$$\begin{aligned} x &= \frac{2\kappa v_0}{y_0} (t - t_0) + O(t^{-1}) \\ y &= y_0 - \frac{\beta}{t} + O(t^{-2}) \end{aligned} \quad (4.13)$$

where  $y_0$ ,  $t_0$ ,  $v_0$ , and  $\beta$  are constants of integration. Of these constants,  $t_0$  simply corresponds to a shift of the zero of time, while  $\beta$  is related to the others by

$$\beta = \frac{y_0(a^2 + y_0^2)}{4\kappa v_0} \frac{B}{E}. \quad (4.14)$$

The meanings of  $v_0$  and  $y_0$  are clarified by writing the asymptotic solution in terms of  $b$  and  $r$ :

$$\begin{aligned} r &= v_0 |t| + \dots \\ b &= \frac{\kappa v_0^2}{y_0^2} t^2 + \dots \end{aligned} \quad (4.15)$$

We see that asymptotically the massive monopoles move with a constant relative velocity  $v_0$ , while  $b$  varies quadratically with time.<sup>10</sup> Substituting this asymptotic solution back into the energy, we find that

---

<sup>10</sup> This would imply that as  $t$  approaches  $\infty$  ( $-\infty$ ), the cloud parameter increases (decreases) at a rate that exceeds the speed of light; we will return to this point below.

$$E = \frac{\mu}{2} \dot{r}^2 + \frac{\kappa}{2} \frac{\dot{b}^2}{b} + \dots . \quad (4.16)$$

As  $t \rightarrow \pm\infty$  the terms indicated by dots vanish, while the two terms shown explicitly tend to constants. These latter two terms can be interpreted as a massive monopole energy  $E_r$  and a cloud energy  $E_b$ , with

$$y_0^2 = a^2 \frac{E_r}{E_b} . \quad (4.17)$$

Because of the multiple mapping of  $b$  and  $r$  into the  $x$ - $y$  plane, for each asymptotic solution in Eq. (4.13) there are seven other physically equivalent solutions that are obtained by reversing the signs of  $x$  or  $y$  or by the interchange of  $x$  and  $y$ .

### B. Joining the asymptotic solutions when $\mathbf{J} = \mathbf{Q} = 0$

Having found the possible asymptotic behaviors, we now want to obtain solutions of Eq. (4.10) for finite times. As with the asymptotic solutions, these will depend on four constants of integration. One of these can be absorbed in a rescaling of  $t$  (with a corresponding rescaling of  $E$  and  $B$ ) and a second in a shift of the zero of time. Hence, the trajectories in the  $x$ - $y$  plane depend nontrivially only on two constants, which we take to be  $B/E$  and  $E_r/E_b$ ; without loss of generality, we can choose the trajectories to begin in the first octant, so that the latter quantity is equal to  $y_0^2/a^2$ . Equations (4.11) and (4.12) can be combined to yield a quadratic equation for  $dy/dx = \dot{y}/\dot{x}$ . The solution of this equation gives  $dy/dx$  as a function of  $x$ ,  $y$ , and  $B/E$ . Hence, two trajectories with the same value of  $B/E$  but different  $y_0$  cannot cross. While our numerical solutions indicate that the same may be true for trajectories with the same  $y_0$  and different  $B/E$ , we have no proof of this statement.

We used numerical integration to obtain solutions for various values of  $y_0$  and  $B/E$ . We will begin by describing our results for  $y_0 = a$  (i.e., initially equal values of  $E_r$  and  $E_b$ ). In Fig. 1, we show some trajectories in the  $x$ - $y$  plane for  $y_0 = a$  and several values of  $B/E$ . Figure 2 shows  $r$  and  $b$  as functions of time for these trajectories. Note that  $r$  and  $b$  have been plotted in units of  $r_c = 2\kappa/\mu$ ; recall that this is approximately equal to the sum of the core radii of the two massive monopoles.

In examining these solutions, it is useful to focus on the points where  $b = r$  (corresponding to crossing one of the 45-degree lines  $x = \pm y$ ) and where  $r = 0$  (corresponding to crossing either of the coordinate axes in the  $x$ - $y$  plane). When  $b = r$ , the cloud is of minimal size,<sup>11</sup>

---

<sup>11</sup>This is not necessarily the minimum value of  $b$ . In most cases  $r < b$  when  $b$  reaches its minimum, so that the smallest value of  $b$  corresponds to a nonminimal cloud.

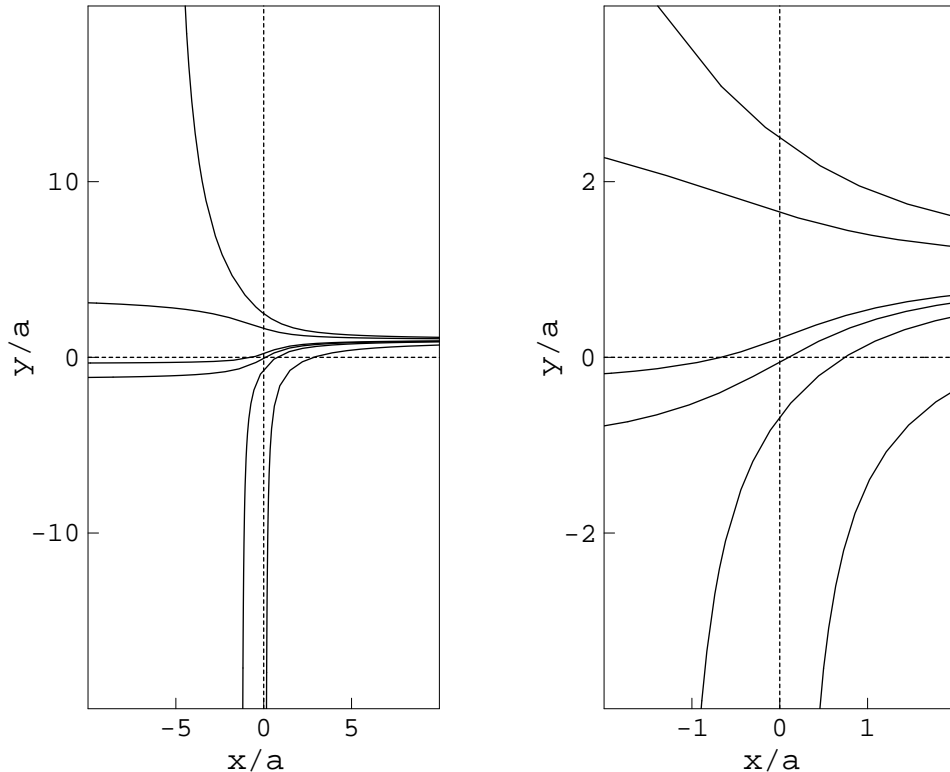


FIG. 1. Several trajectories in the  $x$ - $y$  plane for  $y_0 = a$ . Beginning from the top, these correspond to values of  $B/E$  of  $-1.40$ ,  $-0.60$ ,  $0.66$ ,  $0.85$ ,  $1.20$ , and  $3.00$ . The graph on the right is a blow-up of the region near the origin.

and can be viewed as having shrunk to the line segment joining the massive monopoles. The field configuration is an embedding of a purely Abelian  $SU(3) \rightarrow U(1) \times U(1)$  solution, and the component of the field in the unbroken  $SU(N)$  is a pure dipole field. In terms of massless monopole positions, this corresponds to a configuration where all of the massless monopoles are located on top of one of the massive monopoles. All trajectories pass through at least one such minimal cloud configuration. If  $|B/E| < 1$ , the trajectory passes through two such configurations. Whether  $b = r$  once or twice does not appear to have a dramatic influence on the large time behavior of the solutions.

The points on a trajectory where  $r = 0$  are, of course, the points where the two massive monopoles pass through one another. Since  $x$  and  $y$  both vary monotonically, it is clear that every trajectory must cross at least one coordinate axis and so must have at least one such point. Thus, the two massive monopoles that are approaching each other on a straight line (because  $\mathbf{J} = 0$ ) cannot stop and reverse direction before they meet. However, it is possible for them, after passing through each other once, to stop, reverse direction, pass through each other a second time, and finally emerge with their original direction of motion reversed. Whether this second possibility is realized is determined, for a given  $y_0$ , by  $B/E$ . For  $y_0 = a$ , the monopoles reverse direction if  $0.51 \lesssim B/E \lesssim 2.60$ ; the boundaries of this

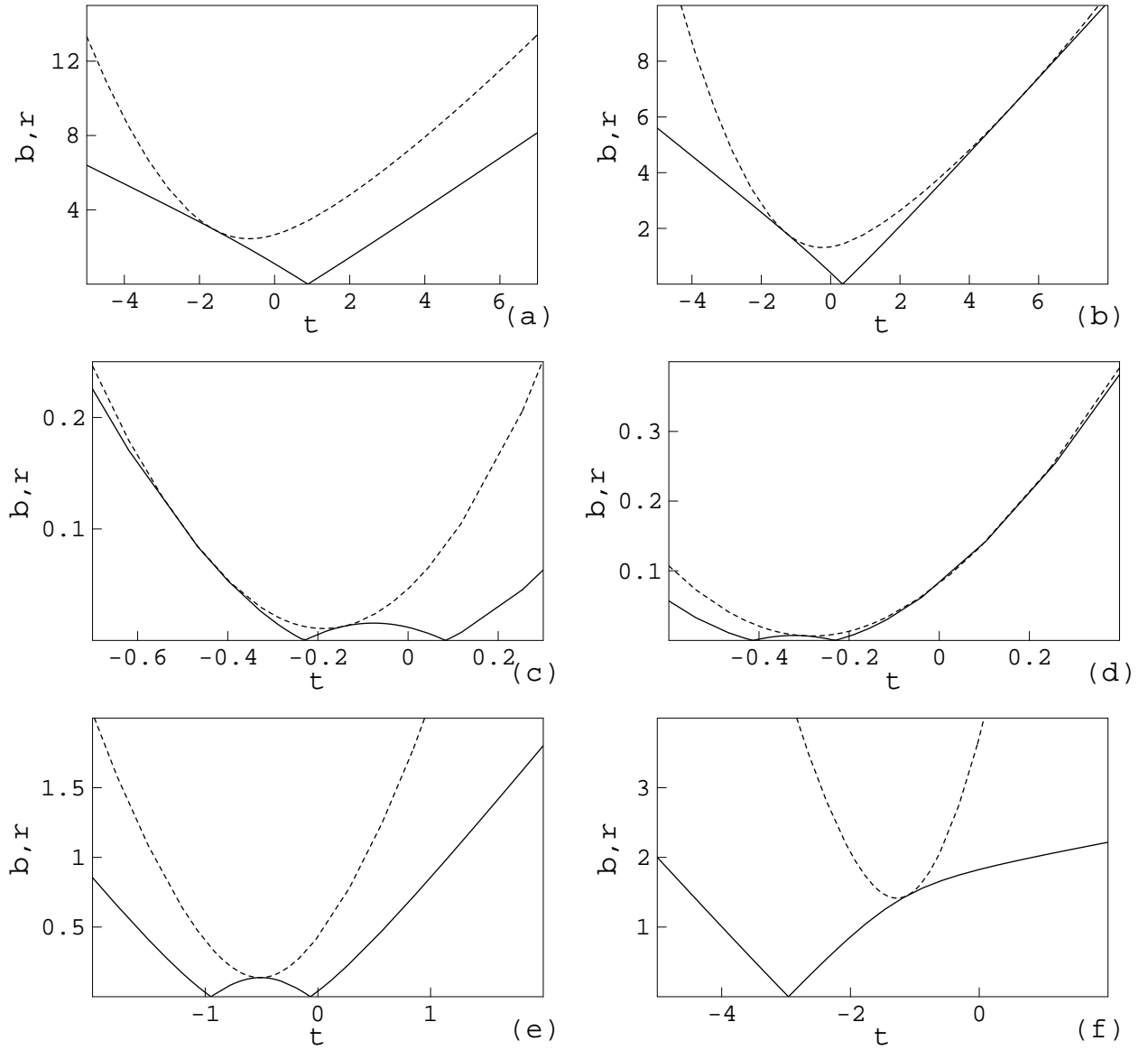


FIG. 2. Plots of  $b$  (dashed line) and  $r$  (solid line) as functions of  $t$  for the trajectories shown in Fig. 1. The progression from (a) to (f) corresponds to moving from top to bottom in Fig. 1. Time is shown in units of  $a/2\sqrt{E}$ , while  $b$  and  $r$  are plotted in units of  $r_c = 2\kappa/\mu$ . Note that the scale varies from plot to plot.

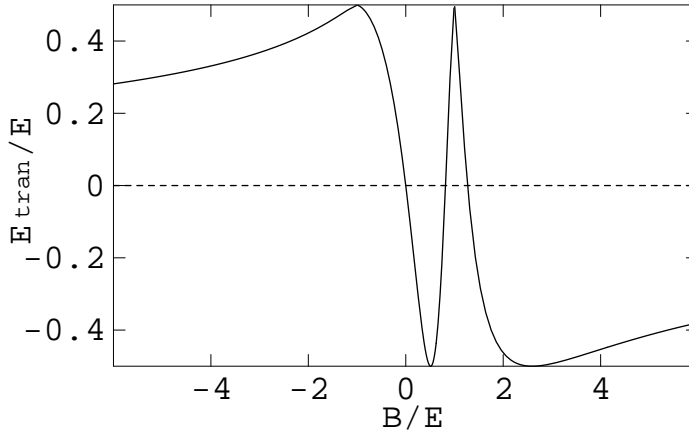


FIG. 3. Energy transfer from the cloud to the massive monopoles as a function of  $B/E$ , for  $y_0 = a$ .

range correspond to solutions where the massive monopole velocities vanish as  $t \rightarrow \infty$ .

The trajectories displayed in Figs. 1 and 2 were chosen to illustrate the various possible behaviors ( $b = r$  once or twice,  $r = 0$  once or twice). Several points should be noted. First, there does not appear to be any particular striking effect when  $r = 0$ . Because  $r$  is by definition positive,  $\dot{r}$  changes sign, but the magnitude of  $\dot{r}$  varies continuously. Similarly,  $b(t)$  shows no unusual behavior when  $r$  vanishes. All this is consistent with our expectations; since the two massive monopoles have no direct interactions, they should be able to pass through each other with little effect.

By contrast, each of the massive monopoles does interact directly with one of the massless monopoles comprising the cloud. This might suggest that there should be a noticeable effect when a massive and a massless monopole position coincide; i.e., when  $b = r$ . On the other hand, the massless monopoles are hardly point particles, since the entire cloud region can be viewed as being composed of the massless cores. Nevertheless, it does seem that the greatest effect on the trajectories occurs when  $b \approx r$ . Thus, the largest changes in the slope of  $r(t)$  coincide almost exactly with the vanishing of  $b - r$ . Note also that the effect of these massive-massless “collisions” seems to be greatest when they occur at small  $b$  and  $r$ . This is perhaps clearest in the trajectories where the interaction is strong enough to reverse the direction of motion of the massive monopoles, so that  $r = 0$  twice. In these cases,  $b$  and  $r$  coincide when  $r$  is so small that the two massive cores overlap each other.

Even when the massive monopoles do not change direction, we can gauge the strength of their interaction with the cloud by the amount of energy transferred between the cloud and the massive monopoles. In Fig. 3 we show this as a function of  $B/E$  for  $y_0 = a$ . Although the details of this plot vary somewhat with  $y_0$ , two points are fixed:

- 1) If  $B/E = 0$ ,  $\dot{y}$  vanishes identically, so  $y$  is constant in time and there is no energy

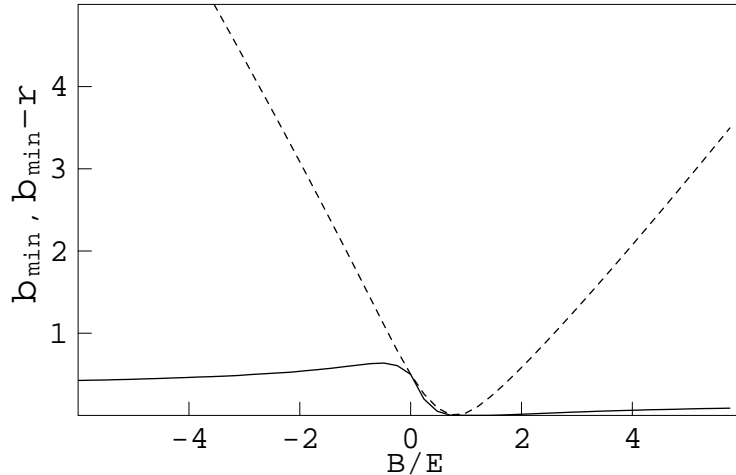


FIG. 4. Minimum cloud parameter  $b_{\min}$  (dashed line) and the corresponding value of  $b_{\min} - r$  (solid line) as functions of  $B/E$ , for  $y_0 = a$ . Both  $b$  and  $r$  are plotted in units of  $2\kappa/\mu$ .

transfer.

2) If  $B/E = \pm 1$ , the trajectory asymptotically approaches one of the lines  $x = \pm y$  at large time, corresponding to a final state with minimal cloud,  $b = r$ . In this case, all of the initial cloud energy is transferred to the massive monopole kinetic energy.

Figure 3 should be compared with Fig. 4, where we we plot the minimum value of  $b$  as a function of  $B/E$ . We see that the largest energy transfers are associated with small values of  $b$ , and that the energy transfer decreases as  $b_{\min}$  increases for  $|B/E| \gg 1$ . In Fig. 4 we have also shown the value of  $b - r$  at the time that  $b$  achieves its minimum. Note that this value is always less than or comparable to the monopole core radius.

We have also studied solutions with  $y_0 = 100a$  (i.e.,  $E_r \gg E_b$ ) and  $y_0 = 0.01a$  ( $E_r \ll E_b$ ). The general picture is very much as for the case of  $y_0 = a$ . The analogues of Figs. 1 and 2 are qualitatively quite similar. We again find that  $b - r$  is small when the cloud parameter  $b$  achieves its minimum size, and the greatest amount of energy transfer between the cloud and the massive monopoles occurs when  $b_{\min}$  is small. One notable difference is found in those  $y_0 = 0.01a$  solutions where the massive monopoles reverse direction. In contrast with the  $y_0 = a$  case, the massive monopoles need not be overlapping at the time of this reversal. This is readily understood. Because the cloud energy is so much greater than the massive monopole energy, relatively little energy transfer is required to reverse the sign of  $\dot{r}$ , and so  $b$  at the time of the collision can be larger than it was in the previous case. This emphasizes that the critical factor for the  $y_0 = a$  reversal was that  $b$  was small; the fact that the massive cores overlapped was coincidental.

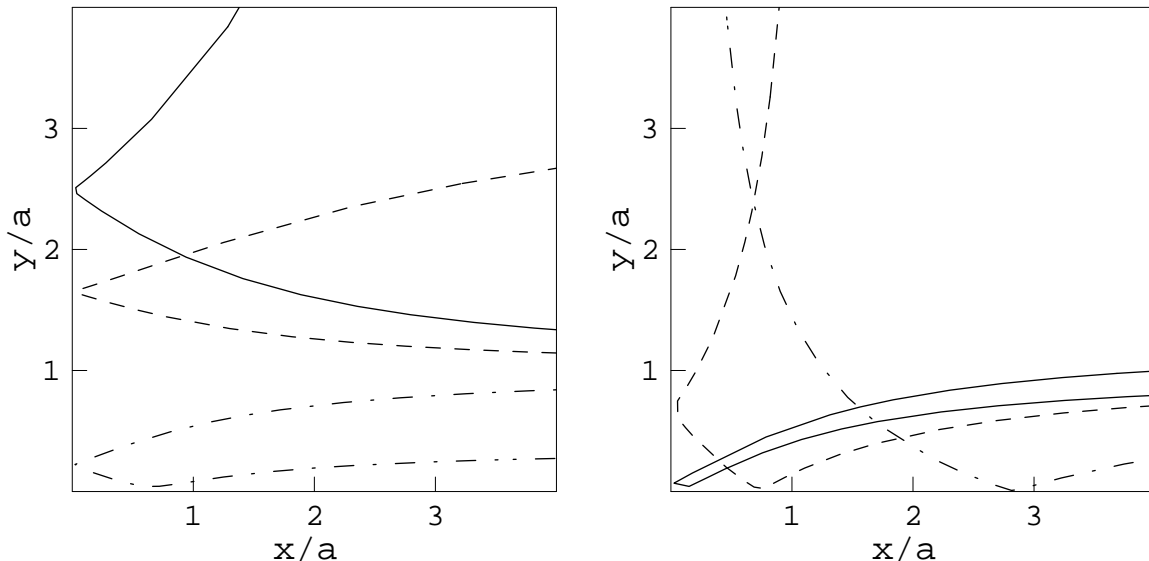


FIG. 5. Several trajectories in the  $x$ - $y$  plane for nonzero  $\mathbf{J}$ . The values of  $y_0$  and  $B/E$  are the same as in Fig. 1, while  $J = 0.001a\sqrt{E}$ . The trajectories in the left box correspond to the top three trajectories in Fig. 1, while those in the right box correspond to the bottom three trajectories in Fig. 1.

### C. Solutions with nonzero $\mathbf{J}$ and $Q$

The effective potential terms in Eq. (4.1) come into play when either  $\mathbf{J}$  or  $Q$  is nonzero. With nonvanishing angular momentum, there is a centrifugal barrier that prevents the vanishing of  $r$ . The trajectory in the  $x$ - $y$  plane cannot cross either axis, and so is confined to a single quadrant. For large  $\mathbf{J}$ , this barrier ensures that  $r$ , and hence  $b$ , is always large, and thus suppresses interactions between the massive monopoles and the cloud. For small but nonzero  $\mathbf{J}$ , the effect of the centrifugal barrier is to make the trajectories appear to reflect off the  $x$ - and  $y$ -axes. We illustrate this in Fig. 5. Except for the value of  $\mathbf{J}$ , the initial data for the trajectories in this figure are the same as for those shown in Fig. 1. Equation (3.19) for  $\mathbf{J}^2$  implies that the motion of the massive monopoles is confined to a plane. In Fig. 6, we illustrate this motion by showing the path of  $\mathbf{r}$  in the plane perpendicular to  $\mathbf{J}$  for one of the trajectories shown in Fig. 5. Note once again that there is little evidence of interaction when the massive monopoles are at their closest approach.

If  $Q \neq 0$ , there is a barrier that forbids the vanishing of  $b - r$ , or equivalently, the crossing of the lines  $x = \pm y$ . When  $Q$  is large,  $b - r$  can never be small, and so there is little interaction among the monopoles. For small nonzero  $Q$ , we find behavior analogous to that for  $\mathbf{J} \neq 0$ , with trajectories appearing to bounce off the lines  $x = \pm y$ .

## V. CONCLUDING REMARKS

In this paper we have studied the properties of the magnetically charged counterparts of the electrically-charged massless particles that arise when a gauge theory is spontaneously

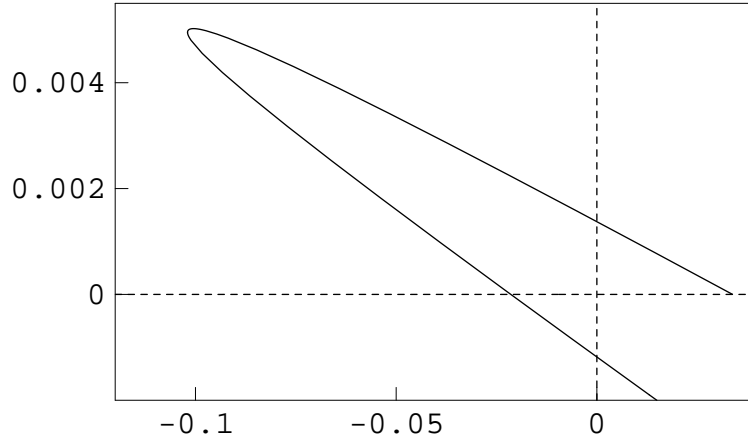


FIG. 6. A portion of the orbit of the massive monopole separation  $\mathbf{r}$  in the plane perpendicular to  $\mathbf{J}$ . Note that the turnaround of the monopole motion does not occur at the time of closest approach. The trajectory shown here corresponds to  $B/E = 1.2$ ,  $y_0 = a$ , and  $J = 0.002a\sqrt{E}$ .

broken to a non-Abelian subgroup. Previous studies of static BPS solutions have shown that these massless monopoles coalesce into a cloud of non-Abelian field surrounding one or more massive monopoles. In the scattering solutions that we have studied, these clouds act very much like thin shells, with a size of order  $b$ , that contract until they collide with and bounce off the cores of the massive monopoles. At large times, when this shell is far from the massive cores, the cloud and the massive monopoles are essentially decoupled, and have separately conserved energies. Their interaction occurs primarily at the time that the shell overlaps the massive cores. We find that the strength of this interaction, as measured, e.g., by the amount of energy transfer, tends to be greatest if  $b$  is small at the time of this overlap.

Further evidence in support of this picture can be obtained from another system that has been studied in some detail. When  $SU(3)$  gauge theory is spontaneously broken to  $SU(2)\times U(1)$  there are two species of fundamental monopoles, one massive and one massless. The Nahm data and moduli space metric for the BPS solutions containing one massless and two massive monopoles were obtained by Dancer [14,15]. These solutions depend on twelve parameters. Ten of these correspond to the center-of-mass position, global  $SU(2)\times U(1)$  phases, and overall spatial rotations. The remaining two,  $k$  and  $D$ , arise as parameters in elliptic functions that enter the Nahm data. These span a geodesic submanifold which, after a nonlinear change of variables to eliminate coordinate singularities in the moduli space metric, is often illustrated as in Fig. 7. (This figure is actually a six-fold covering of the submanifold, completely analogous to our eight-fold mapping of  $b$  and  $r$  onto the  $x$ - $y$  plane.)

The precise relations between position in this figure and cloud size and monopole separation are rather complex, with analytic expressions only known asymptotically [16]. However,



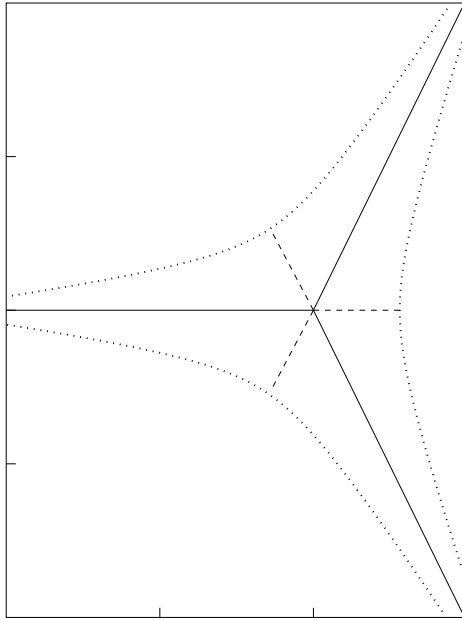


FIG. 7. The two-dimensional Dancer submanifold discussed in the text. The hyperbolic solutions correspond to points on the solid lines, while the trigonometric solutions lie on the dashed lines. The boundaries, indicated by dotted lines, correspond to embedded  $SU(2)$  two-monopole solutions.

the qualitative picture is easily described. Points far out along the three legs of the diagram correspond to solutions containing two well-separated massive monopoles, with the separation increasing with distance along the leg, while points in the central part of the figure correspond to solutions in which the massive monopole cores overlap and deform each other. The boundaries of the figure correspond to embedded  $SU(2)$  two-monopole solutions; in our language, these are solutions with infinite cloud parameter. (These boundaries are infinitely far, in metric distance, from any interior point.) The lines that bisect the legs correspond to special axially symmetric solutions [15]. The solid portions of these lines in Fig. 7 correspond to “hyperbolic solutions” that can be viewed as solutions with minimal cloud (the analogue of our  $b = r$  solutions) and with the separation between the massive monopoles increasing with distance from the center. The dashed portions of these lines correspond to “trigonometric solutions” that are composed of two overlapping massive monopoles and a massless cloud that increases from minimal size at the center to infinite size at the boundary of the figure.

Geodesics on this two-dimensional submanifold correspond to scattering solutions with vanishing angular momentum and internal charges. In contrast to the  $SU(N)$  example we have studied in this paper, there are direct interactions between the two massive monopoles. Consequently, there is nontrivial scattering even when the cloud is infinitely large. Thus, each of the three geodesics that bound the moduli space in Fig. 7 corresponds to a process

in which the two massive monopoles start infinitely far apart, approach head-on, and then recede at right angles to their initial motion; during the entire process the cloud remains infinitely large.

Numerical solutions of the geodesic equations were obtained by Dancer and Leese [17]. Examining these, we see behavior quite consistent with our interpretation of our  $SU(N)$  solutions, in that the interaction between the cloud and the massive monopoles is greater if the massive monopoles are closer together at the time of the minimal cloud configuration. We see this in two ways. First, there are some geodesics that start in one leg of the figure, cross the line of trigonometric solutions and begin to move down another leg, and then, after crossing the line of hyperbolic solutions, cross a second line of trigonometric solutions and exit via third leg. These may be viewed as analogous to the  $SU(N)$  scattering solutions in which the two massive monopoles reverse direction. As with the latter solutions, these “three-leg trajectories” are found only if the massive monopoles are sufficiently close in the minimal cloud configuration; in other words, if the trajectory goes too far down the second leg, the massive monopoles cannot reverse direction.

The effects of cloud interactions on the “two-leg trajectories” that cross a line of hyperbolic solutions but only a single line of trigonometric solutions are more subtle. At large times these trajectories lie between the boundary and the line of hyperbolic solutions, with the cloud size increasing as the relative distance to the boundary decreases. Comparing the distance of the geodesics from the boundary at points equally far down the initial and final legs thus gives a measure of the net interaction between the cloud and the massless monopoles, somewhat analogous to the  $SU(N)$  energy transfer that we plotted in Fig. 3. Examination of the Dancer-Leese geodesics shows that the greatest change between initial and final legs, and thus the greatest interaction, occurs if the geodesic crosses the line of hyperbolic solutions nearest the center of the figure; i.e., nearest the point of minimal massless monopole separation.

Before closing, we must address the validity of the moduli space approximation. There is a potential problem in this regard in any theory where the excitation of massless particle modes is a possibility. The fact that the asymptotic solution of Eq. (4.15) has the cloud parameter  $b$  increasing faster than the speed of light at large times is an indication that there actually is a breakdown of the moduli space approximation in the example we have studied. Considerable insight in this issue can be obtained by studying [18] an  $SO(5)$  example with a spherically symmetric cloud. This symmetry makes it possible to compare the predictions of the moduli space approximation with a numerical solution of the full field equations, starting from a slowly varying initial configuration. It turns out that the moduli space approximation continues to be reliable until  $\dot{b}$  becomes of order unity. After that time, the

edge of the cloud develops into a rather well-defined front expanding outward at the speed of light. Behind this front, in the cloud interior, the time evolution of the fields continues to be well-described by the moduli space solution (i.e., as if  $b \sim t^2$ ). Ahead of the front, the evolution of the fields is much slower, consistent with a slow linear growth of the cloud at a rate fixed by the initial value of  $\dot{b}$ .

How does this affect the picture of monopole-cloud scattering that we have developed? Two cases can be distinguished. In one, a static solution with finite  $r$  and  $b$  is subject to an external disturbance that induces small, but nonzero, values for  $\dot{r}$  and  $\dot{b}$ . As long as  $\dot{b}$  remains small (energy conservation ensures that  $\dot{r}$  will remain small) the moduli space description of the interaction between the cloud and the massive monopoles should be reliable. Eventually  $\dot{b}$  will become of order unity, but since  $r \ll b$  when this happens, the moduli space approximation should continue to give a good description of the subsequent motion of the massive particles. Thus the main modification to our picture is that the velocity of the cloud asymptotically approaches unity, rather than increasing without bound.

In the other case, the initial low-energy configuration approximates a solution with large cloud that is contracting with the magnitude of  $\dot{b}$  being of order unity. We expect that the deviation from the moduli space solution will lead to the emission of long wavelength, low amplitude waves of the massless boson fields that propagate at the speed of light. This will leave behind a configuration whose evolution then proceeds much as in the previous case.

In closing, we note that while our focus in this paper has been on the massless monopole clouds in classical multimonopole configurations, much of the underlying motivation was to gain insight into the states of the electrically-charged elementary particle sector that are dual to these. Thus, it would be of great interest to study the BPS and near-BPS states containing massless and massive elementary particles with non-Abelian charge with the aim of identifying the counterparts of the cloud parameter  $b$  or of the asymptotic separation of the energy between the cloud and the massless monopoles.

## ACKNOWLEDGMENTS

We thank Kimyeong Lee, Changhai Lu, and Piljin Yi for helpful discussions. This work was supported in part by the U.S. Department of Energy.

## APPENDIX A:

In this appendix we show explicitly how to express the metric  $\mathcal{G}_{\text{rel}}$  of Eq.(2.7) in terms of the Euler angles. We restrict ourselves here to the case of  $SU(4) \rightarrow U(1) \times SU(2) \times U(1)$ .

A natural set of parameters is the cloud size  $b$ ; the massive monopole separation  $r$ ; three spatial Euler angles  $\theta$ ,  $\phi$ , and  $\psi$ ; three internal SU(2) Euler angles  $\alpha$ ,  $\beta$ , and  $\gamma$ ; and the relative U(1) phase  $\chi$ . This is a total of nine but, as we discussed in Sec. 2, we only expect eight parameters. We will see later that this conflict is resolved by the identification of a spatial Euler angle with one of the internal SU(2) Euler angles.

The  $z_A^a$  transform as doublets under both the spatial and the internal SU(2), with the upper and lower indices being spatial and internal, respectively. Hence the  $z_A^a$  for arbitrary values of the spatial Euler angles must be of the form

$$\begin{pmatrix} z_A^1 \\ z_A^2 \end{pmatrix} = U(\theta, \phi, \psi) \begin{pmatrix} a_A \\ b_A \end{pmatrix} \quad (\text{A1})$$

where  $a_A$  and  $b_A$  are functions of  $b$ ,  $r$ ,  $\chi$ , and the internal Euler angles. We choose a parameterization of  $U(\theta, \phi, \psi)$  such that

$$z_A^a = a_A v^a + b_A \tilde{v}^a \quad (\text{A2})$$

where

$$\begin{aligned} v^a &= \begin{pmatrix} \cos \frac{\theta}{2} e^{\frac{i}{2}(-\psi-\phi)} \\ \sin \frac{\theta}{2} e^{\frac{i}{2}(-\psi+\phi)} \end{pmatrix} \\ \tilde{v}^a &= \begin{pmatrix} \sin \frac{\theta}{2} e^{\frac{i}{2}(\psi-\phi)} \\ -\cos \frac{\theta}{2} e^{\frac{i}{2}(\psi+\phi)} \end{pmatrix} \end{aligned} \quad (\text{A3})$$

Similarly,  $a_A$  and  $b_A$  can be written as linear combinations of

$$\begin{aligned} u_A &= \begin{pmatrix} \sin \frac{\alpha}{2} e^{\frac{i}{2}(-\gamma+\beta)} \\ \cos \frac{\alpha}{2} e^{\frac{i}{2}(-\gamma-\beta)} \end{pmatrix} \\ \tilde{u}_A &= \begin{pmatrix} \cos \frac{\alpha}{2} e^{\frac{i}{2}(\gamma+\beta)} \\ -\sin \frac{\alpha}{2} e^{\frac{i}{2}(\gamma-\beta)} \end{pmatrix} \end{aligned} \quad (\text{A4})$$

with coefficients that depend only on  $r$ ,  $b$ , and  $\chi$ . By performing a gauge rotation, we can make  $a_A$  proportional to  $u_A$ . We then have

$$z_A^a = A u_A v^a + B \tilde{u}_A \tilde{v}^a + C u_A \tilde{v}^a \quad (\text{A5})$$

The 2 relative phases among  $A, B$  and  $C$  can be absorbed in redefinitions of  $\gamma$  and  $\psi$ . Then, by a redefinition  $A \rightarrow A e^{\frac{i}{2}\chi}$ ,  $B \rightarrow B e^{\frac{i}{2}\chi}$  and  $C \rightarrow C e^{\frac{i}{2}\chi}$ , we can make the  $A, B, C$  all real and non-negative. Equations (2.5) and (2.6) then give the constraints

$$\begin{aligned} A^2 + C^2 &= \frac{1}{2}(b+r) \\ B^2 &= \frac{1}{2}(b-r) \\ BC &= 0 \end{aligned} \quad (\text{A6})$$

These are solved by  $A = \frac{1}{2}\sqrt{b+r}$ ,  $B = \frac{1}{2}\sqrt{b-r}$ ,  $C = 0$ . This gives us

$$\begin{aligned}
z_1^1 &= \left( \sqrt{\frac{b+r}{2}} \sin \frac{\alpha}{2} \cos \frac{\theta}{2} e^{-\frac{i}{2}(\gamma+\psi)} + \sqrt{\frac{b-r}{2}} \cos \frac{\alpha}{2} \sin \frac{\theta}{2} e^{\frac{i}{2}(\gamma+\psi)} \right) e^{\frac{i}{2}(\beta+\chi-\phi)}, \\
z_2^1 &= \left( \sqrt{\frac{b+r}{2}} \cos \frac{\alpha}{2} \cos \frac{\theta}{2} e^{-\frac{i}{2}(\gamma+\psi)} - \sqrt{\frac{b-r}{2}} \sin \frac{\alpha}{2} \sin \frac{\theta}{2} e^{\frac{i}{2}(\gamma+\psi)} \right) e^{\frac{i}{2}(-\beta+\chi-\phi)}, \\
z_1^2 &= \left( \sqrt{\frac{b+r}{2}} \sin \frac{\alpha}{2} \sin \frac{\theta}{2} e^{-\frac{i}{2}(\gamma+\psi)} - \sqrt{\frac{b-r}{2}} \cos \frac{\alpha}{2} \cos \frac{\theta}{2} e^{\frac{i}{2}(\gamma+\psi)} \right) e^{\frac{i}{2}(\beta+\chi+\phi)}, \\
z_2^2 &= \left( \sqrt{\frac{b+r}{2}} \cos \frac{\alpha}{2} \sin \frac{\theta}{2} e^{-\frac{i}{2}(\gamma+\psi)} + \sqrt{\frac{b-r}{2}} \sin \frac{\alpha}{2} \cos \frac{\theta}{2} e^{\frac{i}{2}(\gamma+\psi)} \right) e^{\frac{i}{2}(-\beta+\chi+\phi)}. \tag{A7}
\end{aligned}$$

Notice that  $\gamma$  and  $\psi$  always come together in the combination  $\gamma + \psi$ . This is a manifestation of the axial symmetry of this configuration: for any spatial axial rotation that changes the parameter  $\psi$ , one can do an opposite axial gauge rotation that changes  $\gamma$ , so that the metric is invariant.

Substituting these relations into the Eq. (2.7) gives

$$\begin{aligned}
\mathcal{G}_{\text{rel}} &= \left( \frac{1}{2}\mu + \frac{\kappa}{2} \frac{b}{b^2 - r^2} \right) dr^2 + \frac{\kappa}{2} \frac{b}{b^2 - r^2} db^2 - \kappa \frac{r}{b^2 - r^2} dbdr \\
&+ \frac{1}{2}(\mu r^2 + \kappa b)(\sigma_1^2 + \sigma_2^2) + \frac{1}{2}\kappa b(\tau_1^2 + \tau_2^2) + \kappa\sqrt{b^2 - r^2}(-\sigma_1\tau_1 + \sigma_2\tau_2) \\
&+ \frac{\kappa}{2} \left( b - \frac{\mu r^2}{\kappa + \mu b} \right) (\sigma_3 + \tau_3)^2 - \frac{\kappa^2 r}{\kappa + \mu b} (\sigma_3 + \tau_3) d\chi + \frac{\kappa^2 b}{2(\kappa + \mu b)} d\chi^2 \tag{A8}
\end{aligned}$$

where

$$\begin{aligned}
\sigma_1 &= -\sin \psi d\theta + \cos \psi \sin \theta d\phi, \\
\sigma_2 &= \cos \psi d\theta + \sin \psi \sin \theta d\phi, \\
\sigma_3 &= d\psi + \cos \theta d\phi, \tag{A9}
\end{aligned}$$

and

$$\begin{aligned}
\tau_1 &= -\sin \gamma d\alpha + \cos \gamma \sin \alpha d\beta, \\
\tau_2 &= \cos \gamma d\alpha + \sin \gamma \sin \alpha d\beta, \\
\tau_3 &= d\gamma + \cos \alpha d\beta, \tag{A10}
\end{aligned}$$

are the left-invariant one-forms for the rotational and internal SU(2)'s, respectively.

There are several interesting limits of this metric. If the relative distance between the two massive monopoles  $\mathbf{r}$  and the relative U(1) charge  $Q$  both vanish, it reduces to the metric for one massive and one massless monopole in SO(5) [4,12]:

$$\mathcal{G}_{\text{SO}(5)} = \frac{\kappa}{2} \left[ \frac{db^2}{b} + b(\tau_1^2 + \tau_2^2 + \tau_3^2) \right]. \quad (\text{A11})$$

In the limit where we have minimal cloud  $b = r$  and vanishing internal  $\text{SU}(2)$  charges, we get the metric for two distinct massive  $\text{SU}(3)$  monopoles [11]. The angles  $\psi$  and  $\gamma$  can be absorbed into a redefinition of  $\chi$ , and we obtain

$$\mathcal{G}_{\text{SU}(3)} = \frac{1}{2} \left( \mu + \frac{\kappa}{r} \right) \left[ dr^2 + r^2(\sigma_1^2 + \sigma_2^2) \right] + \frac{\kappa^2}{2} \frac{r}{\kappa + \mu r} (-d\chi + \cos\theta d\phi)^2. \quad (\text{A12})$$

We can also consider the limit where  $\mu$  is much greater than both  $\kappa/b$  and the initial energy of the cloud. To leading order, the massive monopole motion decouples from that of the cloud, and we may set  $\dot{\mathbf{r}} = 0$ . Making the change of variables  $b = \frac{u^2}{4}$  and  $r = \frac{\zeta}{2}$ , we get the Eguchi-Hanson [19] metric<sup>12</sup>.

$$\mathcal{G}_{\text{EH}} = \frac{\kappa}{2} \left\{ \frac{du^2}{1 - \frac{4\zeta^2}{u^4}} + \frac{u^2}{4} \left[ \tau_1^2 + \tau_2^2 + \left( 1 - \frac{4\zeta^2}{u^4} \right) \tau_3^2 \right] \right\}. \quad (\text{A13})$$

When  $\zeta = 0$ , this reduces to Eq. (A11).

In order to study the classical dynamics for the general case with nonzero angular momenta and internal charges, it is most convenient to first eliminate the redundant parameters. This can be done, e.g., by simply choosing  $\psi = 0$ . We then write the angular part of the metric as

$$\mathcal{G}_{\text{ang}} = I_{ij}(r, b) \omega^i \omega^j, \quad (\text{A14})$$

where the  $\omega_i$  ( $i = 1, \dots, 6$ ) are one-forms expressed in terms of the various rotational and gauge angles. These satisfy an algebra of the form

$$d\omega^i = \frac{1}{2} C_{jk}^i \omega^j \wedge \omega^k. \quad (\text{A15})$$

where the  $C_{jk}^i$  are antisymmetric in  $j$  and  $k$ . We then define the charges to be  $X_i = I_{ij} \omega^j$ . Using Eq. (A15), we can write the angular equations of motion for Eq. (A14) as

$$\frac{d}{dt} X_i + C_{ki}^j (I^{-1})^{kl} X_j X_l = 0. \quad (\text{A16})$$

Ordinarily, we could have chosen the  $\omega^j$  to include the three  $\sigma_a$  and the three  $\tau_a$ . However, after eliminating the redundant angular variable, this is not possible. Instead, we choose

$$\omega^1 = -\sin\theta d\phi, \quad \omega^2 = d\theta, \quad \omega^3 = \tau_1,$$

---

<sup>12</sup>We thank Kimyeong Lee for pointing this out to us.

$$\omega^4 = \tau_2, \quad \omega^5 = \tau_3 + \cos \theta d\phi, \quad \omega^6 = d\chi. \quad (\text{A17})$$

With this choice, the  $C_{jk}^i$  are not constants, as they are in more familiar examples. The nonzero  $C_{jk}^i$  are given by

$$\begin{aligned} C_{21}^1 &= C_{41}^3 = C_{13}^4 = \cot \theta \\ C_{45}^3 &= C_{53}^4 = C_{21}^5 = C_{34}^5 = 1. \end{aligned} \quad (\text{A18})$$

$I_{ij}$  can be obtained from Eq. (A8) for the metric. It is a block diagonal matrix formed by three two-by-two blocks, with the first two blocks being identical. It is straightforward to verify that Eq. (A16) implies that the square of the angular momentum, Eq. (3.19), and the square of the internal SU(2) charge, Eq. (3.20), are indeed constant.

## REFERENCES

- [1] C. Montonen and D. Olive, Phys. Lett. **72B**, 117 (1977); H. Osborn, Phys. Lett. **83B**, 321 (1979).
- [2] E.B. Bogomol'nyi, Sov. J. Nucl. Phys. **24**, 449 (1976); M.K. Prasad and C.M. Sommerfield, Phys. Rev. Lett. **35**, 760 (1975).
- [3] E.J. Weinberg, Nucl. Phys. **B167**, 500 (1980).
- [4] E.J. Weinberg, Phys. Lett. **B119**, 151 (1982).
- [5] E.J. Weinberg, Nucl. Phys. **B203**, 445 (1982).
- [6] A. Abouelsaood, Phys. Lett. **125B**, 467 (1983); P. Nelson, Phys. Rev. Lett. **50**, 939 (1983); P. Nelson and A. Manohar, Phys. Rev. Lett. **50**, 943 (1983); A. Balachandran, G. Marmo, M. Mukunda, J. Nilsson, E. Sudarshan, and F. Zaccaria, Phys. Rev. Lett. **50**, 1553 (1983); P. Nelson and S. Coleman, Nucl. Phys. **B237**, 1 (1984).
- [7] E.J. Weinberg and P. Yi, Phys. Rev. D **58**, 046001 (1998).
- [8] N.S. Manton, Phys. Lett. **110B**, 54 (1982).
- [9] K. Lee, E.J. Weinberg, and P. Yi, Phys. Rev. D **54**, 6351 (1996).
- [10] N.S. Manton and T.M. Samols, Phys. Lett. B **215**, 559 (1988); D. Stuart, Commun. Math. Phys. **166**, 149 (1994).
- [11] K. Lee, E. Weinberg, and P. Yi, Phys. Lett. B **376**, 97 (1996); J.P. Gauntlett and D.A. Lowe, Nucl. Phys. **B472**, 194 (1996); S.A. Connell, *The dynamics of the SU(3) charge (1,1) magnetic monopoles*, University of South Australia preprint.
- [12] K. Lee, E.J. Weinberg, and P. Yi, Phys. Rev. D **54**, 1633 (1996).
- [13] M.K. Murray, J. Geom. Phys. **23**, 31 (1997); G. Chalmers, *Multi-monopole moduli spaces for SU(N) gauge group*, ITP-SB-96-12, hep-th/9605182.
- [14] A.S. Dancer, Commun. Math. Phys. **158**, 545 (1993).
- [15] A.S. Dancer, Nonlinearity **5**, 1355 (1992).
- [16] P. Irwin, Phys. Rev. D **56**, 5200 (1997).
- [17] A.S. Dancer and R.A. Leese, Proc. R. Soc. London **A440**, 421 (1993).
- [18] X. Chen, H. Guo, and E.J. Weinberg, in preparation.
- [19] T. Eguchi and A.J. Hanson, Ann. Phys. (N.Y.) **120**, 82 (1979).